Protein Science (1997), 6:1237–1247. Cambridge University Press. Printed in the USA.

Secondary and tertiary structural changes in γδ resolvase: Comparison of the wild-type enzyme, the I110R mutant, and the C-terminal DNA binding domain in solution

BORLAN PAN,[1] ZHENGWU DENG,[2] DINGJIANG LIU,[3] SUSMITA GHOSH,[1] AND GREGORY P. MULLEN[1]

[1]University of Connecticut Health Center, Department of Biochemistry, Farmington, Connecticut 06032

(RECEIVED December 26, 1996; ACCEPTED March 10, 1997)

Abstract

γδ Resolvase is a site-specific DNA recombinase (M_r 20.5 kDa) in *Escherichia coli* that shares homology with a family of bacterial resolvases and invertases. We have characterized the secondary and tertiary structural behavior of the cloned DNA binding domain (DBD) and a dimerization defective mutant in solution. Low-salt conditions were found to destabilize the tertiary structure of the DBD dramatically, with concomitant changes in the secondary structure that were localized near the hinge regions between the helices. The molten tertiary fold appears to contribute significantly to productive DNA interactions and supports a mechanism of DNA-induced folding of the tertiary structure, a process that enables the DBD to adapt in conformation for each of the three imperfect palindromic sites. At high salt concentrations, the monomeric I110R resolvase shows a minimal perturbation to the three helices of the DBD structure and changes in the linker segment in comparison to the cloned DBD containing the linker. Comparative analysis of the NMR spectra suggest that the I110R mutant contains a folded catalytic core of ~60 residues and that the segment from residues 100 to 149 are devoid of regular structure in the I110R resolvase. No increase in the helicity of the linker region of I110R resolvase occurs on binding DNA. These results support a subunit rotation model of strand exchange that involves the partial unfolding of the catalytic domains.

Keywords: DNA; folding; interaction; NMR; protein; recombination; resolvase; structure

γδ Resolvase (M_r 20.5 kDa) is a site-specific DNA recombinase in *Escherichia coli* that shares homology with a family of resolvases and invertases in a variety of bacteria (Grindley & Reed, 1985). The structure of resolvase can be divided into three distinct regions, consisting of a catalytic domain (residues 1–120), a DNA binding domain (residues 149–183), and a linker region between the two globular domains. Limited proteolysis of γδ resolvase yields a C-terminal 43-residue fragment (5 kDa) with DNA binding activity and an N-terminal 140-residue fragment (15.5 kDa) with oligomerization and catalytic functions. The structure of the catalytic domain has been determined by X-ray crystallography (Sanderson et al., 1990) and displays a mixed antiparallel/parallel β-sheet surrounded by helices denoted A–E. A pair of parallel E-helices (residues 100–120) provides the contacts in adjacent monomers. Although previous structures of resolvase have revealed the overall configuration of the dimerized form, the catalytic mechanism of resolvase is not well understood due to the distant location of the active site from the DNA cleavage site (Yang & Steitz, 1995).

The solution structure of the resolvase DBD generated by proteolysis has been determined previously by NMR spectroscopy (Liu et al., 1994). The proteolytically generated DBD consists of three helices, with helix-1 and helix-3 crossing in a right-handed manner. Helix-2 and helix-3 form a helix-turn-helix motif, while an amino-terminal arm connected to helix-1 is flexible in solution. It has been suggested, based on a lack of electron density for the DBD in the intact enzyme and the presence of electron density while bound to DNA, that DNA binding induces and stabilizes the fold of the DBD and the linker connecting the catalytic domain (Yang & Steitz, 1995). Previous NMR results provided evidence that the hydrophobic core of the DBD was intact in the WT dimer resolvase (Liu et al., 1994) as do proteolysis experiments. DNA-induced folding of the resolvase DBD (Yang & Steitz, 1995) is in

Reprint requests to: Gregory P. Mullen, Department of Biochemistry MC3305, University of Connecticut Health Center, Farmington, Connecticut 06032; e-mail: gmullen@panda.uchc.edu.

[2]Present address: Department of Chemistry, Vanderbilt University, Nashville, Tennessee 37235.

[3]Present address: Department of Medical Biophysics, University of Toronto, Toronto, Ontario, Canada M5G 2M9.

Abbreviations: WT, wild type; I110R, Ile-110 to Arg-110 mutation; V114R, Val-114 to Arg-114 mutation; DBD, DNA binding domain; HSQC, heteronuclear single-quantum correlated spectroscopy; TOCSY, total correlation spectroscopy; NOESY, NOE spectroscopy.

apparent contradiction to our results that showed that the isolated DBD is a folded and stable structure in solution (Liu et al., 1994).

To investigate the roles of solution structural flexibility in DNA binding and recombination, the secondary and tertiary structural behavior of the cloned DBD and a dimerization defective mutant in solution were characterized. We have investigated the folding behavior of the DBD in the isolated state, in the I110R monomeric resolvase, and in the WT resolvase, and relate these properties to the DNA binding process. The I110R and V114R mutants were constructed to disrupt helix dimerization of the catalytic domain and, as expected, were found to behave as monomers at the concentrations used in gel mobility shift assays and gel filtration analysis (Hughes et al., 1993). The monomeric form of resolvase is likely to represent a functional intermediate in the strand exchange process according to the subunit rotation model (Stark et al., 1989, 1991). NMR analysis was performed for the domains in the I110R resolvase and a comparative structural characterization of the monomeric protein is presented.

Results

Native molecular weight determinations

The oligomerization states of the resolvase mutants were determined by gel filtration HPLC. The retention time for the I110R mutant yields a molecular weight of 23.6 ± 1.4 kDa at all protein concentrations studied. Thus, the I110R mutant was monomeric at concentrations ≤0.925 mM. At a concentration of 1.1 mM, the retention time for the V114R resolvase mutant yields a molecular weight of 21 kDa. The V114R mutant was therefore monomeric at the highest concentration studied and is not expected to change from this state at lower protein concentrations.

To determine whether the I110R monomer can associate with the WT resolvase dimer, HPLC studies were performed on a 1:1 mixture of the WT resolvase and the I110R mutant (Fig. 1). At low concentrations (<0.05 mM), only monomers were present. At higher concentrations (>0.08 mM), the monomeric and dimeric states coexisted. These results indicate that the WT resolvase forms dimers at higher protein concentrations, whereas the I110R mutant remains monomeric. As indicated by the presence of the monomeric form at high concentrations, heterodimers can be ruled out because, at the highest concentration of the mixtures, a constant concentration of the monomeric species (I110R) was observed. Heterodimers would have resulted in a shift of the monomeric species toward the dimeric species, as found for the WT resolvase. Interactions at a second dimerization interface do not occur under these conditions.

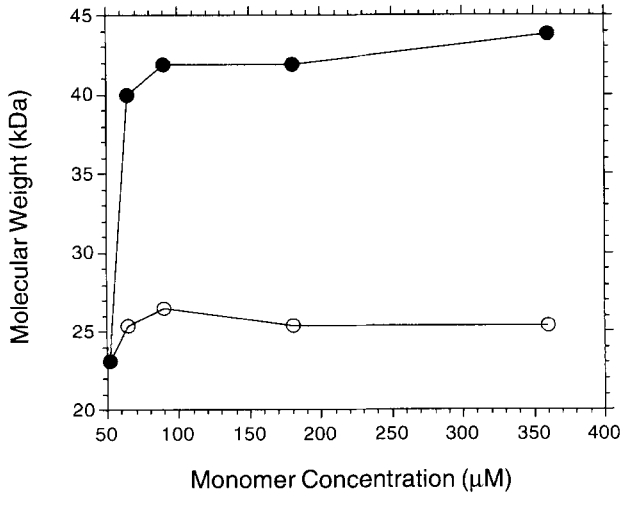

Fig. 1. HPLC-determined molecular weights of an equimolar mixture of resolvase I110R (○) and WT resolvase (●) as a function of protein monomer concentration.

Sequential assignments of the cloned resolvase DBD

The ^{1}H-^{15}N HSQC spectrum (Fig. 2) of the cloned resolvase DBD (residues 115–183) displays well-resolved amide peaks. Sequential resonance assignments for the DBD have been made using standard procedures (Wüthrich, 1986) by establishing the connectivity patterns in 3D ^{1}H-^{15}N TOCSY-HSQC and 3D ^{1}H-^{15}N NOESY-HSQC spectra. With the exception of residues 115–117, the amide proton and ^{15}N resonances have been assigned for all residues. Triple-resonance HNCA and HN(CO)CA experiments (Grzesiek & Bax, 1992) were used to verify the backbone assignments. The amide proton assignments were compared to those made previously for the proteolytically generated DBD (residues 141–183). Sequential $d_{NN(i,i+1)}$ and $d_{\alpha N(i,i+1)}$ connectivities, medium-range $d_{NN(i,i+2)}$, $d_{\alpha N(i,i+2)}$, $d_{\alpha N(i,i+3)}$ connectivities, and the $^{13}C_{\alpha}$ chemical shift indices (Wishart & Sykes, 1994) within the α helical segments (D149–Q157, S162–T167, and R172–N183) show that the α-helices are similarly present in the cloned resolvase DBD (Fig. 3). A strip plot taken from the 3D ^{1}N-^{15}N HSQC-NOESY spectrum illustrates the NOEs for residues D147–Q157 (Fig. 4A).

In contrast to the three helices of the DBD, residues 118–148 of the linker region do not display connectivities indicative of well-defined structural elements (Fig. 4B). The random coil nature of this region is supported by the presence of strong NOEs and/or exchange cross peaks to water, the lack of strong $d_{NN(i,i+1)}$ or

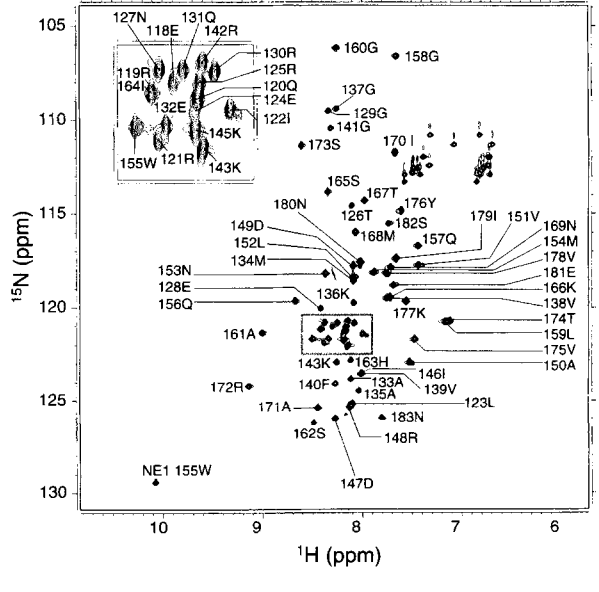

Fig. 2. ^{1}H-^{15}N HSQC spectrum of the resolvase 69-mer in 1 M ammonium sulfate, 5 mM Tris-d_{11}, pH 6.9. Amino acid residue assignments are indicated.

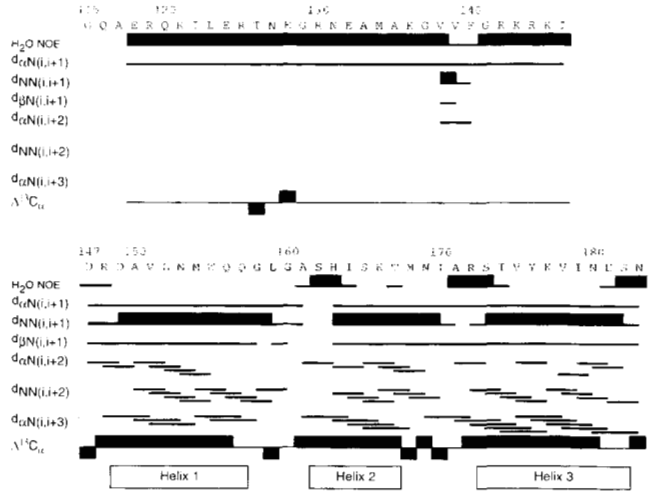

Fig. 3. Summary of NOE connectivities for the ^{15}N-labeled cloned resolvase DBD including short- and medium-range NOEs, $^{13}C_\alpha$ chemical shift indices, and the elements of secondary structure. NOE intensities are taken from the 200-ms mixing time 3D ^{1}H-^{15}N NOESY-HSQC.

medium-range connectivities, and the agreement of the $^{13}C_\alpha$ chemical shifts with the random coil values. NOE/exchange cross peaks to water are not observed (or only weakly) for residues within the helices (Figs. 3, 4). An exception to the overall random coil character of the linker region occurs at residues 138–140, where $d_{NN(i,i+1)}$ and medium-range connectivities occur.

Effects of ammonium sulfate concentration on the structure of the DBD

γδ Resolvase is limited in solubility at low salt concentrations. We have characterized the folded state of the resolvase DBD by 1D NMR in solutions ranging from 100 mM to 1 M ammonium sulfate (Fig. 5). An X-ray structure of the DBD could not be obtained at ~1 M ammonium sulfate due to missing electron density (Rice & Steitz, 1994). Because of the limited solubility, the protein concentration used in these experiments was approximately 0.15 mM. In solutions containing 1 M ammonium sulfate, sharp methyl proton resonances are observed at −0.23 and 0.06 ppm, and have been assigned to the γ and δ methyl protons of I179. The upfield chemical shifts result from interaction with the aromatic ring of W155. At ammonium sulfate concentrations below approximately 400 mM, the resonances were broadened and less intense. As the ammonium sulfate concentration was increased above 400 mM, the methyl resonances intensified and were shifted upfield.

To further investigate the cause of structural perturbation at low salt concentrations, we measured ^{1}H-^{15}N HSQC spectra of the resolvase DBD at 400 and 300 mM ammonium sulfate (Fig. 6). In 1 M ammonium sulfate, ^{1}H-^{15}N cross peaks for all amides within residues 147–183 have been assigned. In 400 mM ammonium sulfate, cross peaks for the following backbone amides were weak or missing: 155–159, 161–163, 168–170, 172, 173, 176, 179, and 182. At 300 mM, additional cross peaks corresponding to the following residues were missing: 164, 166, 174, 177, 178, 180, and 181. At 400 mM ammonium sulfate, the structural perturbations are located at the C-terminal residues of helix-1, at both ends of helix-2, and at several residues throughout helix-3 (Fig. 7A). Two of these perturbed regions near the amino ends of helix-2 and helix-3 also correspond to regions displaying NOE cross peaks to water (Fig. 7B). Another group of the perturbed peaks correspond to residues that contribute to hydrophobic packing. At 300 mM ammonium sulfate, perturbations occur throughout the C-terminal portion of the DBD after residue 155.

CD spectra of the cloned resolvase DBD shows that the secondary structure is largely similar at low and high ammonium sulfate concentrations (Fig. 8A). A difference in the helicity, corresponding to approximately 26% or six helical residues, was observed between samples of the cloned DBD at 1 M and 100 mM ammonium sulfate. Thus, there was some degree of secondary structure loss at low-salt conditions, but the general secondary structure was retained. A similar difference in the helicity of I110R compared with the cloned DBD was observed between samples containing 1 M and 100 mM ammonium sulfate (Fig. 8A). A cooperative increase in helicity of the DBD as detected by the molar ellipticity at 220 nm (Fig. 8B) was observed as the ammonium sulfate concentration was titrated from 100 mM to 1 M. The increase in the molar ellipticity displays hysteresis due to the incomplete reformation of the helical structure upon increasing the salt concentration after the solution is diluted to 100 mM ammonium sulfate. Upon binding the cloned DBD to the 14-mer dsDNA half site, a slight increase in the helical content was observed and corresponded to a helicity of the DBD alone in approximately 400 mM ammonium sulfate (not shown). No significant increase in the helicity of the I110R was observed upon binding to the 14-mer dsDNA half site (not shown).

Folded states of the DBD and the catalytic domain in the resolvase I110R

A comparison of the folded state of the cloned resolvase DBD and the comparable polypeptide chain of the I110R was performed using 2D ^{1}H-^{15}N HSQC, 3D ^{1}H-^{15}N TOCSY-HSQC, and 3D ^{1}H-^{15}N NOESY-HSQC spectra. The folded state of the catalytic domain was assessed from these spectra. As expected, the ^{1}H-^{15}N HSQC spectrum of resolvase I110R (Fig. 9A) contains a greater number of peaks than that of the isolated DBD and linker segment polypeptide. The assigned peaks from the resolvase DBD in 1 M ammonium sulfate ^{1}H-^{15}N HSQC were mapped on the resolvase I110R ^{1}H-^{15}N HSQC spectrum to determine any differences in the chemical shifts. Only small differences between the resolvase DBD and the resolvase I110R chemical shifts were observed in the three helices of the DBD. It is evident from the weak intensity and lack of dispersion of peaks in the ^{1}H-^{15}N HSQC spectra that some regions in I110R exist in a disordered state in solution. A ^{1}H-^{15}N HSQC spectrum of I110R in 2 M NaCl at pH 7.6 shows a significant transition in the intensities and dispersion of the peaks. At pH 7.6, a significant portion of the DBD peaks, particularly those corresponding to the linker region, disappear as a result of an apparent proteolytic cleavage within the linker, as determined by SDS-PAGE, and increased amide proton exchange rates (Fig. 9B). However, ~60 of the remaining catalytic domain peaks become more intense with better resolved line widths. The increase in the resolution of the remaining peaks indicates that a core structure of the catalytic domain forms a stable fold.

The connectivities for the cloned DBD and I110R are similar for helices 1, 2, and 3, as illustrated for helix 1 (Fig. 10). The DBD displays the same structural features in the resolvase I110R as in the cloned and proteolytically generated resolvase DBD. However, there appears to be significant differences for several residues of

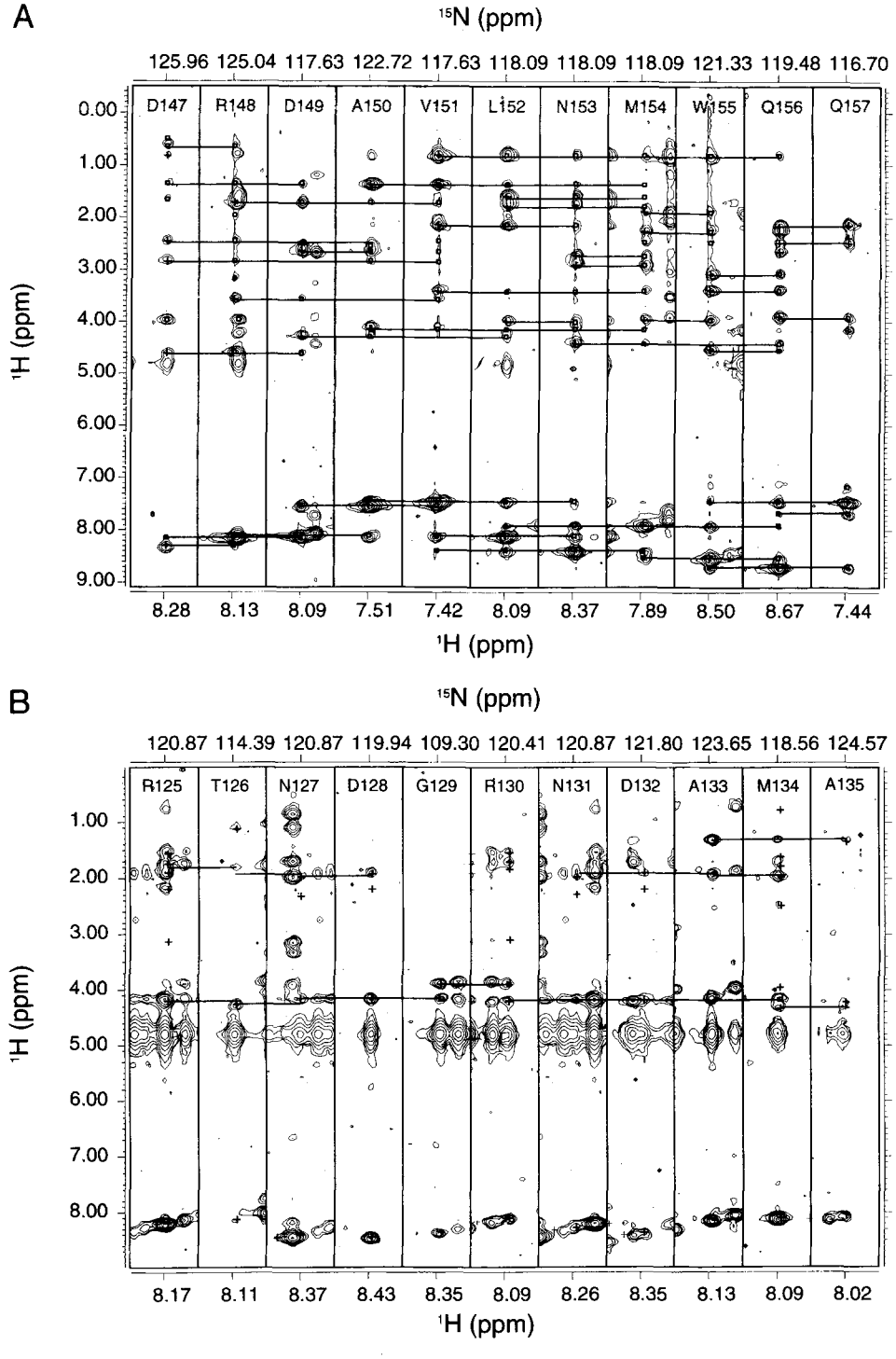

Fig. 4. Composite strips from the 200-ms 3D ^{1}H-^{15}N NOESY-HSQC spectrum of the ^{15}N-labeled cloned DBD showing sequential connectivities within residues 147–157 encompassing helix-1 (**A**) and within the random coil region of residues 125–135 (**B**). Each panel is taken from an ^{15}N plane in the 3D spectrum at the assigned ^{15}N and NH chemical shifts for the designated residue. Lines indicate sequential and medium-range connectivities.

the linker region. In particular, the segment from residues E118 to E128 shows several missing peaks in the resolvase I110R ^{1}H-^{15}N HSQC spectrum.

The lack of NOE connectivities and the presence of NOE or exchange cross peaks to water indicate that residues 118–147 are disordered in the linker attached to the DBD. In the I110R mutant, the segment from residues 118 to 128 does not appear to exist in the same microenvironment as in the cloned resolvase DBD, as seen by the different ^{1}H-^{15}N spectral fingerprint for resolvase I110R compared with the linker segment of the cloned DBD. The

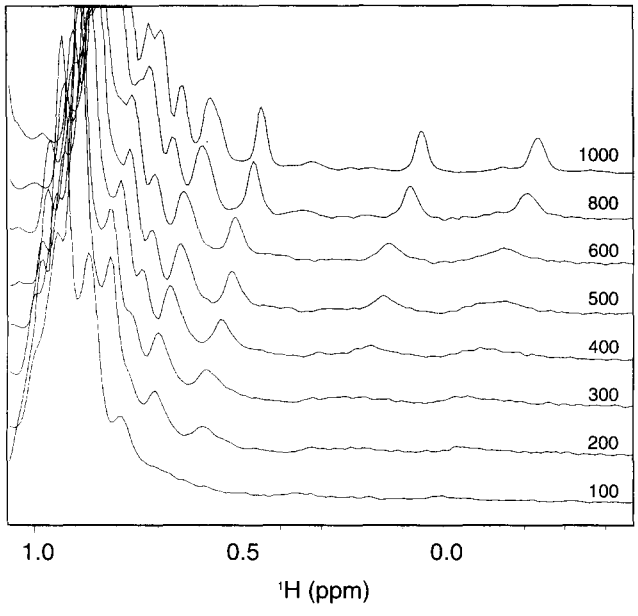

Fig. 5. Effects of ammonium sulfate concentration (indicated in mM) on the upfield region of the 1D ^{1}H spectra of the cloned DBD.

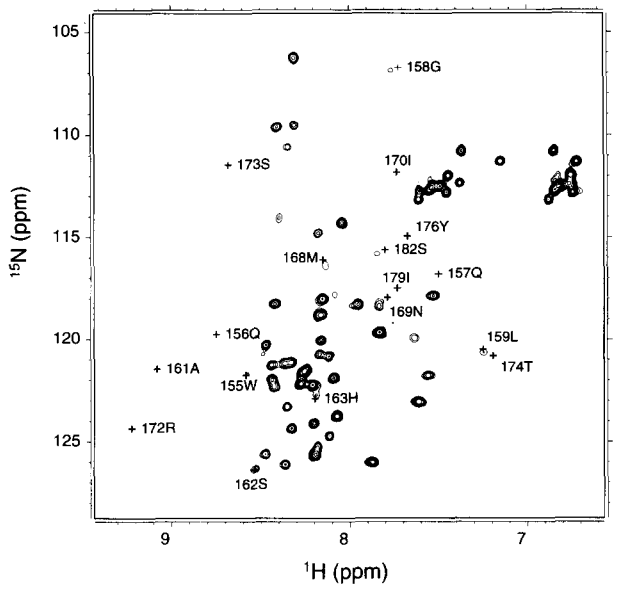

Fig. 6. ^{1}H-^{15}N HSQC spectrum of the cloned DBD in 400 mM ammonium sulfate. Residues that are missing from the cloned resolvase DBD at this salt concentration are indicated with (+) and the residue numbers.

changes in the ^{1}H-^{15}N HSQC spectra of the linker segment may result from interactions or electrostatic effects of the neighboring catalytic domain, or may be associated with more ordered structure in the I110R resolvase. Smaller chemical shift differences for residues 129–146 indicate that these residues are similarly disordered in both the I110R resolvase and the cloned resolvase DBD. The CD results show no dramatic increase in helicity for I110R resolvase on binding DNA, as seen similarly for the cloned resolvase DBD containing the linker segment. Together with the results obtained by ^{1}H-^{15}N HSQC, the CD results indicate that the linker segment (residues 118–128) in I110R resolvase remains nonhelical in the presence of DNA.

NMR comparison of the I110R mutant and the WT resolvase

Comparison of the aromatic region of the 2D NOESY spectra of the I110R and WT resolvase (Fig. 11) shows that many of the aromatic cross peaks display nearly identical chemical shifts, including those of Y176 and W155 in the DBD. The line widths are narrower for the I110R, consistent with the monomeric state and the decreased correlation time. Many of the aromatic cross peaks for the catalytic domain in the I110R spectrum are found similarly in the WT spectrum. However, at least five cross peaks are present in the WT spectrum, but are missing from or shifted significantly in the I110R spectrum. There is also one strong upfield aromatic cross peak that is present in the I110R spectrum that is not seen in the WT spectrum. Several weaker cross peaks are present in the WT spectrum that are not observed in the I110R spectrum at the 100-ms mixing time.

Differences between I110R and the WT resolvase for the aromatic resonances appear to result from changes in the packing interactions with the affected dimerization helix, because no aromatic residues are in the dimerization helix and the closest aromatics that could be affected are F92 and F140. The less than predicted number of cross peaks (~60 of 120) in the ^{1}H-^{15}N fingerprint for I110R resolvase catalytic domain indicate a substantial number of residues that are unfolded or disordered.

Discussion

Flexibility of the DNA binding and catalytic domains of resolvase in solution

The most important conclusion that can be drawn from this work is that both domains in γδ resolvase are highly flexible in solution and that multiple folding/unfolding events play significant roles in DNA binding and crossover during recombination. Under physiological salt concentrations, γδ resolvase exhibits partially folded tertiary structure within the DBD, whereas the catalytic domain of the monomeric resolvase appears to retain a folded core structure consisting of approximately 60 residues. As a monomer, the I110R resolvase is likely to mimic the physiological state of the enzyme and a subunit rotation intermediate during recombination. In the unbound and monomeric state, γδ resolvase displays a molten tertiary structure within the DBD, an apparent absence of the dimerization helix-E and the associated D-helices, an unfolded linker segment connecting the domains (residues 121–140) and little increase in the helicity on binding DNA. Because WT resolvase is a monomer at physiological concentrations, the results also indicate that the dimerization helix is formed after binding of two monomers to the *res* sites. The results for I110R suggest that the dimerization helices and associated linker region (residues 121–140) connecting the catalytic domain to the DBD become unfolded during recombinational crossover between adjoining dimers at the two *res* recombination sites.

Importance of flexibility in the DBD

We have concentrated part of this study on the structural flexibility of the DBD and whether observations of missing electron density

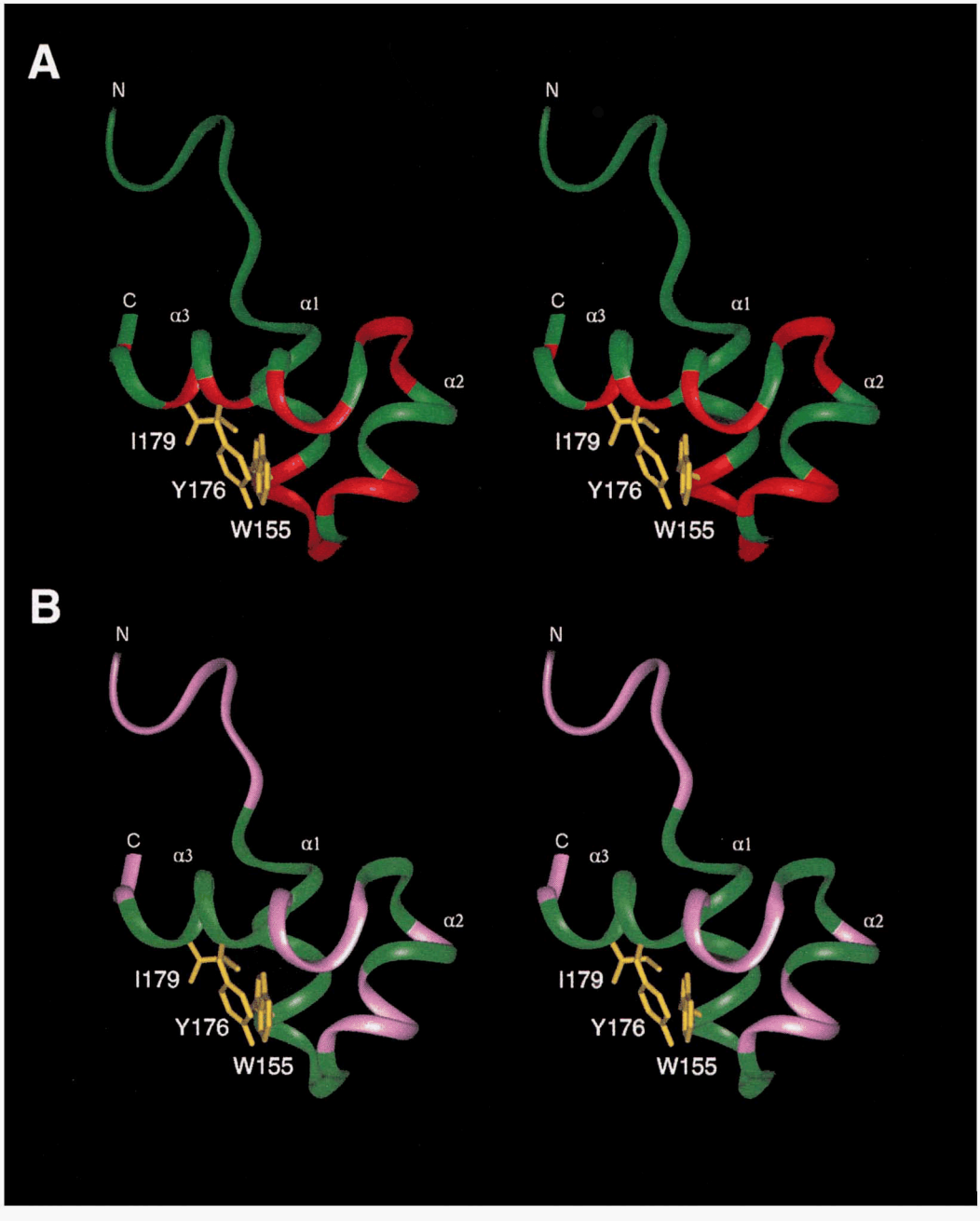

Fig. 7. Secondary and tertiary structural perturbations in the resolvase DBD under low-salt conditions and water NOE/exchange cross peaks shown for the average NMR solution structure (1RES). **A:** Residues that are perturbed at 400 mM ammonium sulfate are marked in red on the ribbon structure. Residues responsible for the hydrophobic packing of residue I179 are shown in yellow. Alpha helices 1, 2, and 3 are indicated by α1, α2, and α3. **B:** Amide protons of the resolvase DBD displaying NOE cross peaks to water are shown in magenta.

by X-ray could be verified in solution. What physiological significance could such flexible structure have? We find that the tertiary structure is molten in the DBD at physiological salt concentrations, but the secondary structure is intact. DNA-induced folding of tertiary structure within the DBD on interaction at the imperfect palindromic sequences within sites I, II, and III likely results in the most effective means of binding more than one sequence. The differences in the ^{1}H-^{15}N correlations for the DBD under low-salt conditions are indicative of unfolded tertiary structure resulting from decreased hydrophobic interactions.

The predominant changes in tertiary structure observed in the resolvase DBD (Fig. 7) lead to a localized secondary structure disruption near the amino ends of helix-2 and helix-3. Direct evidence for loss of the hydrophobic interaction between the γ and δ methyl groups of I179 in helix-3 and the aromatic ring of W155 in helix-1 was found by observation of broadened and downfield-shifted methyl resonances of I179 in the 1D spectra at decreasing ammonium sulfate concentrations. Essentially all DNA binding affinity determined previously for resolvase results from the DNA interaction of the DBD (Abdel-Meguid et al., 1984) and helix-2–

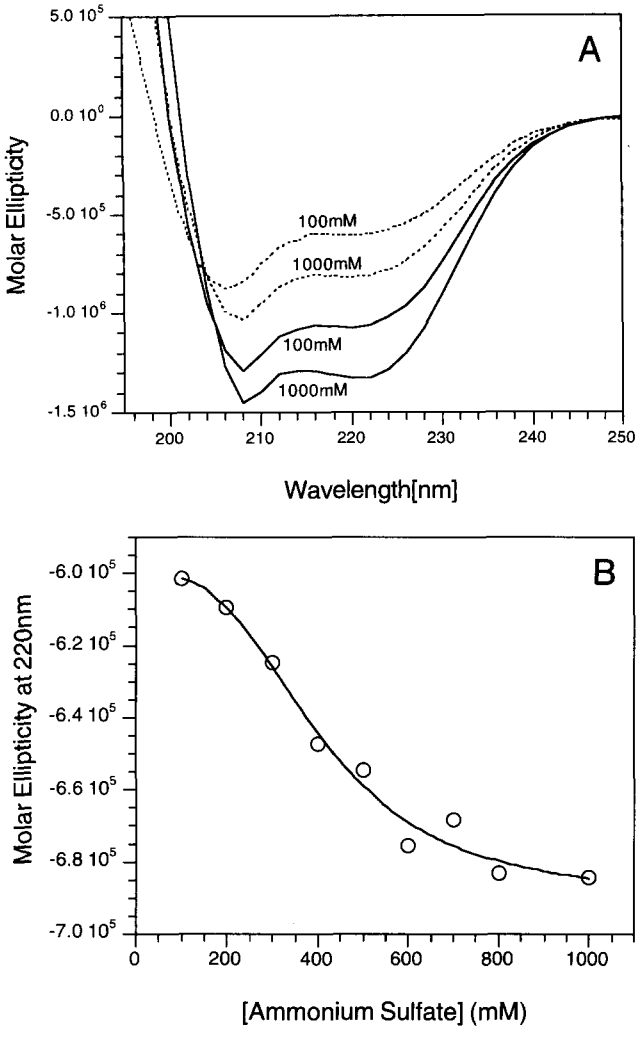

Fig. 8. Effect of ammonium sulfate concentration on the CD spectra of cloned resolvase DBD and I110R. **A:** Spectra of the cloned DBD (dashed curves) and resolvase I110R (solid curves) in 100 and 1,000 mM ammonium sulfate. **B:** Increase in alpha helical content of the cloned resolvase DBD as monitored by the molar ellipticity at 220 nm with increasing ammonium sulfate concentration.

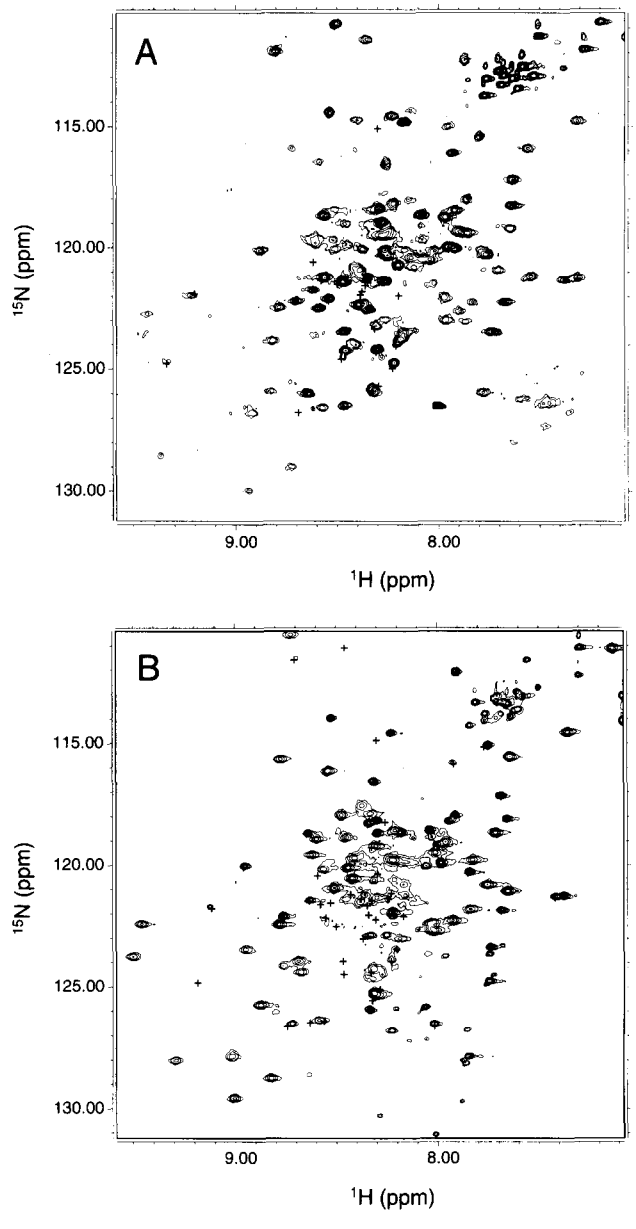

Fig. 9. A: One region of the ^{1}H-^{15}N HSQC spectrum of the resolvase I110R in 1 M ammonium sulfate, 5 mM Tris-d_{11}, pH 6.9. **B:** Central region of the ^{1}H-^{15}N HSQC spectrum of the resolvase I110R mutant in 2 M NaCl, 5 mM Tris-d_{11} at pH 7.6 after cleavage in the linker. Positions of the cloned DBD cross peaks are indicated (+).

turn–helix-3 forms the helix–turn–helix DNA binding motif in resolvase. Y176 in helix-3 closes off the hydrophobic core (Fig. 7) and makes a phosphate contact in the DNA complex and a hydrophobic contact at a thymine-methyl group. These interactions would stabilize the hydrophobic core of the DBD and allow helix-3 to adjust in the structure in a manner that is dependent on the DNA binding site.

The DNA-induced folding of the resolvase DBD appears to indicate conformational adaptability upon DNA binding and provides a mechanism for the range of specific functions that resolvase must assume. Resolvase first forms an ordered synaptic complex involving sites II and III that is distinguishable from the configuration occurring at site I (Watson et al., 1996). To accomplish this, specific interactions must be formed at the three different sequences of varying lengths. Recent investigations have shown that the deviations from perfect inverted-repeat symmetry in the resolvase binding sites lead to the ordered binding of subunits and induces structural asymmetry (Blake et al., 1995). This structural plasticity appears to tailor the structure of the resolvase complex at each site for a particular function during synapsis and recombination. A similar situation is observed in the *trp* repressor, where the coupling of protein folding to DNA binding apparently optimizes the specificity of binding to various sites (Gryk et al., 1996). The disordered tertiary structure seen in the resolvase DBD thereby allows specific binding configurations at each DNA binding site.

Importance of flexibility in the catalytic domain

The catalytic domain of the I110R mutant appears to consist of a relatively stable catalytic core along with regions of severe struc-

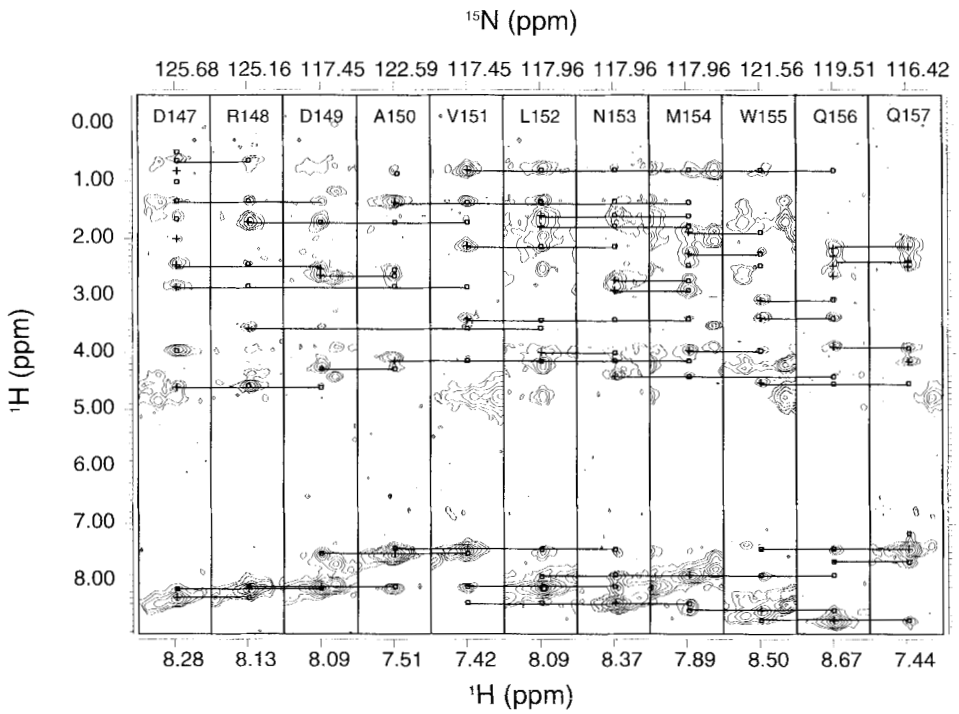

Fig. 10. Composite strips from the 70-ms 3D ^{1}H-^{15}N NOESY-HSQC spectrum of the ^{15}N-labeled I110R resolvase in 1 M ammonium sulfate, 5 mM Tris-d_{11}, pH 6.9, showing sequential connectivities within residues 147–157 that form helix-1.

tural disorder. The results are consistent with chymotrypsin digestion of the WT dimeric resolvase in which fragments of 15 kDa and 5 kDa have been isolated (corresponding to cleavage at F140). On further digestion of the catalytic domain with trypsin, a 10-kDa fragment has been isolated that apparently corresponds to cleavage at a lysine near F92 (Abdel-Meguid et al., 1984). Thus, the catalytic core structure likely resides within residues 1–92. Changes in the aromatic 2D NOESY spectrum between I110R and WT resolvase are in part due to structural differences at F92 and F140.

The subunit rotation model for strand exchange (Stark et al., 1989) is the most direct interpretation accounting for the topological changes occurring during recombination. In this model, a pair of subunits on the left side of a covalently linked tetramer makes a 180° right-handed rotation relative to the subunits on the right side. Because the available crystal structures of the catalytic domain do not suggest a mechanism whereby this rotation could occur without permanent dissociation, an alternative model was proposed where crossover was achieved through relatively small

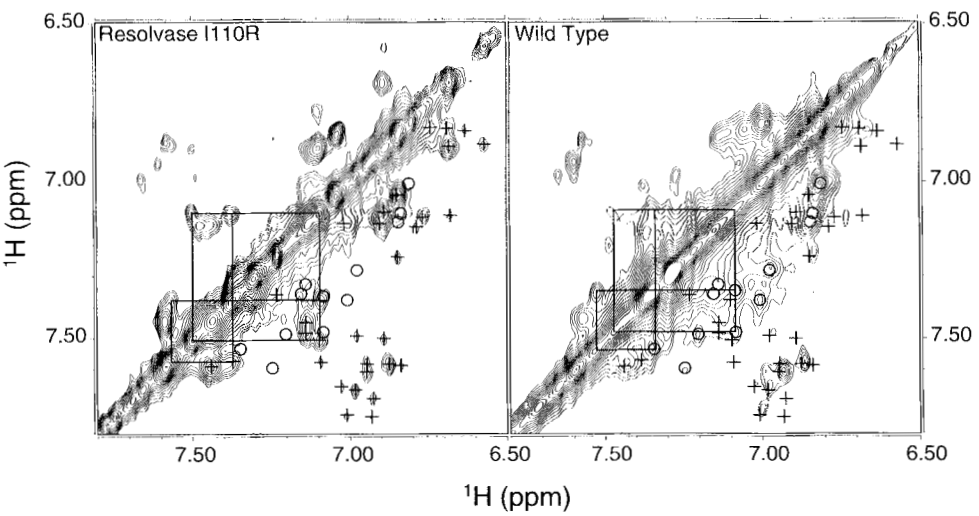

Fig. 11. Aromatic region of the 2D NOESY spectrum of the resolvase I110R and WT resolvase showing positions of cross peaks present in the I110R spectrum (+) and additional peaks present in the WT resolvase (○). The W155 spin system is shown.

localized changes in the conformation of the DNA (Rice & Steitz, 1994). However, recent crosslinking experiments have demonstrated that recombination is effective with the DBD covalently bound to the ends of the DNA half-site (McIlwraith et al., 1996). Because the center of the crossover site is attached covalently to the catalytic Ser-10 in the intermediate (Boocock et al., 1995), each subunit and its associated half-site apparently exchange together.

The results presented here suggest a mechanism for the subunit rotation model that reconciles these contradictory observations. The disordered structure present in the I110R resolvase domain demonstrates that a high degree of conformational disorder exists in the catalytic domain and that this conformational flexibility is coupled to the dissociation of the dimer interface. The structural disorder present in the catalytic domain suggests that, in these regions, novel contacts could occur that are able to facilitate a concerted subunit exchange. A model for DNA crossover based on these results entails an unfolding of the catalytic domains upon phosphodiester bond cleavage. This process could coincide with the dissociation of the initial dimer pair and concomitant reassociation with the adjoining subunits mediated through novel interactions in the unfolded regions. The partially unfolded tetrameric species could then re-fold to form new complementary dimer interfaces. During this process, resolvase dimers bound at *res* sites II and III of the synaptosome presumably functions in abutting resolvase dimers bound at each *res* site I. The remarkable flexibility in resolvase appears to function not only in adapting the molecule to specific functions at particular DNA binding sites, but also in dynamically mediating the catalytic strand exchange process.

Materials and methods

Plasmids

The WT resolvase protein was overexpressed in the AR120 *E. coli* strain from the plasmid pGH286 (Hatfull et al., 1989). The I110R and V114R mutants of γδ resolvase were overexpressed in the AR120 *E. coli* strain from pRH57 and pNG264 (Hughes et al., 1993). The γδ resolvase and mutant proteins were purified as described previously (Hatfull et al., 1989). For ^{15}N-labeling of the I110R resolvase, the mutant gene was subcloned into a T7 overexpression vector pET23 (Novagen) at the *Nde* I site within the ATG start codon. An *Nde* I–*Nde* I fragment (790 bp) containing the mutant tnpR gene was isolated after *Nde* I restriction digestion of pRH57 and inserted into the *Nde* I digested pET23 vector. The direction of the insert was determined by *Pvu* I digestion of the resulting plasmid pDJ1, which contains *Pvu* I sites near the 5′ end of the gene and in the pET23 vector. Expression of the 21-kDa polypeptide corresponding to I110R resolvase was confirmed by SDS-PAGE analysis after IPTG induction in the BL21/DE3 strain. The C-terminal DBD containing the linker segment (69 residues) was overexpressed in the BL21/DE3 *E. coli* strain from the plasmid pNG380 (a gift from Prof. Nigel Grindley).

Protein purification

The WT and mutant resolvase proteins were purified as described previously (Hatfull et al., 1989). Attempts at using the AR120 cell line for overproduction of ^{15}N-labeled resolvase in minimal media were unsuccessful. pDJ1 was used for IPTG-induced overexpression of the II110R resolvase in a minimal media supplemented with vitamins and $^{15}NH_4Cl$ (Weber et al., 1992) in the BL21/DE3 strain containing the accessory plasmid pLysS (Novagen). The cell culture was grown at 37 °C and IPTG was added after the optical density at 600 nm reached 0.9–1.0. Further growth continued for an additional 3–4 h. The purification protocol was essentially as described previously, except for the following modifications. After sonication of the cells in buffer containing 20 mM Tris, pH 8.0, 10 mM $MgCl_2$, and 5 mM β-mercapto ethanol (TMB), the insoluble fraction was extracted into 8 M urea. This extract was dialyzed against 2 M NaCl TMB, followed by dialysis against TMB. The precipitated resolvase was collected, extracted into 6 M urea TMB, and fractionated on a fast-flow CM-sepharose (Pharmacia) column (42 × 1.5 cm). Approximately 50 mg of purified ^{15}N-labeled I110R resolvase was obtained from 1 L of cell culture.

Minimal media growth and induction of the BL21/DE3 cells harboring the plasmids pLysS and pNG380 for overproduction of the cloned C-terminal resolvase DBD (residues 115–183) followed the procedure described above for the I110R resolvase. Purification of the resolvase DBD was essentially the following modification of an unpublished procedure (Prof. N. Grindley, pers. comm.). After induction by IPTG (0.4 mM) for 3–4 h, the cells were harvested by centrifugation. The cell pellet was suspended in 10 mM Tris, pH 7.2, 100 mM NaCl, and 5 mM EDTA (TNE) and, after centrifugation, ammonium sulfate was added to bring the supernatant to 65% saturation. All purification procedures were performed at 0–5 °C. The pellet obtained after centrifugation was suspended with dissolution in TNE and the solution was dialyzed against 100-fold excess TNE for 4 h. The dialyzed solution was loaded immediately onto a fast-flow CM-sepharose column and was eluted with a linear gradient of 100 mM to 1 M NaCl in 10 mM Tris, pH 7.2. The resolvase DBD eluted at approximately 300 mM NaCl. Fractions containing >90% purity of the DBD were pooled to yield approximately 50 mg from a 1-L culture.

Size-exclusion HPLC

Native molecular weight determination of the WT γδ resolvase, the I110R and V114R mutants was performed in 10 mM Tris, pH 7.5, 500 mM NaCl by size-exclusion HPLC on an ABI 151A system using a Bio-Sil SEC125 size-exclusion column (Bio Rad). Protein absorbance was detected at 280 nm. Molecular weight standards from Bio Rad (thyroglobulin, bovine gamma globulin, chicken ovalbumin, myoglobin, and vitamin B_{12}) were used to construct a plot of log (molecular weight) versus K_{av}.

CD measurements

CD measurements were performed on a JASCO 715 spectropolarimeter using a 0.1-cm cuvette. Samples of the resolvase DBD and I110R were prepared at protein concentrations of 24 μM and 15 μM, respectively, in 100 mM and 1,000 mM ammonium sulfate and 0.5 mM Tris, pH 7.0. The resolvase DBD in 100 mM ammonium sulfate, 0.5 mM Tris, pH 7.0 was titrated by the addition of aliquots of 3 M ammonium sulfate. The initial volume was 200 μL and the final volume after titration was 290 μL. Concentrations of ammonium sulfate in the sample were 100, 200, 300, 400, 500, 600, 700, 800, and 1,000 mM. The mean residue molar ellipticity was calculated by taking into account the dilution of the protein. The alpha helical content of the protein sample was estimated from the molar ellipticity at 220 nm and was fit as a function of the ammonium sulfate concentration to the equation:

$$y = 1/\{1 + (1/K_{eq})[(NH_4)_2SO_4]^n\}, \quad (1)$$

where y is the fraction of helix content between the maximum and minimum, K_{eq} is an equilibrium constant for secondary structure folding, and n is a cooperativity number. A 14-mer site I oligonucleotide (5′-TGTGCGATAATTTA-3′) sequence was added to the resolvase DBD and I110R in 100 mM ammonium sulfate. The final concentration of dsDNA used in the sample was 30 μM. Difference CD spectra of samples with and without DNA were used for comparison to spectra of samples containing only protein.

NMR experiments

The 2D ^{1}H-^{15}N HSQC spectra and the 3D ^{1}H-^{15}N TOCSY-HSQC and ^{1}H-^{15}N NOESY-HSQC spectra were collected using samples containing ~1 mM resolvase I110R or resolvase DBD in 90% H_2O/10% D_2O, 1 M ammonium sulfate at pH 6.9. The 2D NOESY spectra were acquired on samples containing ~1 mM resolvase I110R or WT $\gamma\delta$ resolvase in 99.8% D_2O, 1 M ammonium sulfate at pD 6.9. For studying the effects of ammonium sulfate concentration on the resolvase DBD (115–183), the NMR samples contained 0.15 mM DBD in 90% H_2O/10% D_2O, pH 6.9, and ammonium sulfate concentrations of 100, 200, 300, 400, 500, 600, 800, and 1,000 mM.

2D and 3D NMR spectra were acquired at 500 and 600 MHz on Varian Unity-plus spectrometers. Proton pulses were generated with the observe transmitter and proton amplifiers using channel 1, and high-power and low-power ^{15}N pulses were generated using channel 3. Water suppression was achieved using an on-resonance low-power presaturation for 1D and 2D NOESY and by gradient methods for the 2D ^{1}H-^{15}N HSQC (Kay et al., 1992) and the 3D ^{1}H-^{15}N NOESY-HSQC and 3D ^{1}H-^{15}N TOCSY-HSQC sequences (Zhang et al., 1994). ^{1}H sweep widths were set to 8,000 Hz and ^{15}N sweep widths were set from 1,800 to 2,500 Hz.

For the 2D experiments, 2,048 complex points were collected in the t_2 dimension and 512 complex t_1 increments were collected using the States-TPPI method for phase-sensitive detection (Marion et al., 1989). The 2D NOESY (Kumar et al., 1980) experiments used a 100-ms mixing time with a 5-ms homospoil at the start and a 5-ms homospoil after a composite 180° pulse in the center of the mixing period. Sensitivity enhanced 2D ^{1}H-^{15}N HSQC (Kay et al., 1992) spectra using z-gradients for coherence selection were acquired with 256 complex t_1 increments.

Sensitivity-enhanced 3D ^{1}H-^{15}N NOESY-HSQC and 3D ^{1}H-^{15}N TOCSY-HSQC were acquired using z-gradients for ^{1}H-^{15}N coherence selection (Zhang et al., 1994). For 3D experiments, 512 complex points were collected in t_3, 128 complex points were collected in t_1, and 32 complex points were collected in t_2. The 3D ^{1}H-^{15}N NOESY-HSQC spectra used mixing times of 200 ms for the resolvase 69-mer and 70 ms for the resolvase I110R. The 3D ^{1}H-^{15}N TOCSY-HSQC was a modification of the 3D ^{1}H-^{15}N NOESY-HSQC, which used the DIPSI spin lock as described in the TOCSY-HMQC sequence (Clore & Gronenborn, 1991). The ^{1}H-^{15}N TOCSY-HSQC sequence included a 90° pulse before the mixing period to rotate transverse magnetization to the Z-axis and a delay of 8 ms to remove rotating frame NOEs. ^{15}N decoupling in t_2 and t_3 for 2D and 3D spectra, respectively, used GARP. ^{15}N decoupling in t_1 for 3D spectra was performed by application of a 180° ^{15}N pulse in the center of the evolution period. ^{1}H-^{15}N TOCSY-HSQC spectra were acquired at mixing times of 50 and 70 ms. For the HN(CO)CA experiment (Grzesiek & Bax, 1992), 512 complex points were collected in t_3, 64 complex points were collected in t_1, and 32 complex points were collected in t_2. For the HNCA experiment (Grzesiek & Bax, 1992), 512 complex points were collected in t_3, 32 complex points were collected in t_1, and 32 complex points were collected in t_2.

Multidimensional NMR data were processed with Felix 95.0 (Biosym Technologies) on a Silicon Graphics Indigo 2 workstation. Squared sine bell window functions with shifts of 90° and, in alternate processing, squared sine bell window functions with shifts of 90° and exponential multiplication of 2 Hz, were used in processing the data. A sine bell window function shifted by 60° or 90° was used for the t_2 dimension in 3D spectra. Linear prediction of the first point and twofold zero filling were used for the evolution time-dependent dimensions. Processed NMR spectra were analyzed within the program XEASY (Bartels et al., 1995).

Acknowledgments

This work was supported by the National Institutes of Health grant GM48607.

References

Abdel-Meguid SS, Grindley NDF, Templeton NS, Steitz TA. 1984. Cleavage of the site-specific recombination protein, $\gamma\delta$ resolvase: The smaller of the two fragments binds DNA specifically. *Proc Natl Acad Sci USA 81*:2001–2005.

Bartels C, Xia T, Billeter M, Güntert P, Wüthrich K. 1995. The program XEASY for computer-supported NMR spectral analysis of biological macromolecules. *J Biomol NMR 6*:1–10.

Blake DG, Boocock MR, Sherratt DJ, Stark WM. 1995. Cooperative binding of Tn3 resolvase monomers to a functionally asymmetric binding site. *Curr Biol 5*:1036–1046.

Boocock MR, Xuewei Z, Grindley NDF. 1995. Catalytic residues of $\gamma\delta$ resolvase act *in cis*. *EMBO J 14*:5129–5140.

Clore GM, Gronenborn AM. 1991. Two-, three-, and four-dimensional NMR methods for obtaining larger and more precise three-dimensional structures of proteins in solution. *Annu Rev Biophys Chem 20*:29–63.

Grindley NDF, Reed RR. 1985. Transpositional recombination in prokaryotes. *Annu Rev Biochem 54*:863–896.

Gryk MR, Jardetzky O, Klig LS, Yanofsky C. 1996. Flexibility of DNA binding domain of *trp* repressor required for recognition of different operator sequences. *Protein Sci 5*:1195–1197.

Grzesiek S, Bax A. 1992. Improved 3D triple-resonance NMR techniques applied to a 31 kDa protein. *J Mag Res 96*:432–440.

Hatfull GF, Sanderson MR, Freemont PS, Racciua PR, Grindley NDF, Steitz TA. 1989. Preparation of heavy-atom derivatives using site-directed mutagenesis. *J Mol Biol 208*:661–667.

Hughes RE, Rice PA, Steitz TA, Grindley NDF. 1993. Protein–protein interactions directing resolvase site-specific recombination: A structure function analysis. *EMBO J 12*:1447–1458.

Kay LE, Keifer P, Saarinen T. 1992. Pure absorption gradient enhanced heteronuclear single quantum correlation spectroscopy with improved sensitivity. *J Am Chem Soc 114*:10663–10665.

Kumar A, Ernst RR, Wüthrich K. 1980. A two-dimensional nuclear Overhauser enhancement (2D NOE) experiment for the elucidation of complete proton–proton cross-relaxation networks in biological macromolecules. *Biochem Biophys Res Commun 95*:1–6.

Liu T, DeRose EF, Mullen GP. 1994. Determination of the structure of the DNA binding domain of $\gamma\delta$ resolvase in solution. *Protein Sci 3*:1286–1295.

Marion D, Ikura M, Tschudin R, Bax A. 1989. Rapid recording of 2D NMR spectra without phase cycling: Application to the study of hydrogen exchange in proteins. *J Magn Reson 48*:286–292.

Mcllwraith MJ, Boocock MR, Stark WM. 1996. Site-specific recombination by Tn3 resolvase, photocrosslinked to its supercoiled DNA substrate. *J Mol Biol 260*:299–303.

Rice PA, Steitz TA. 1994. Model for a DNA-mediated synaptic complex suggested by crystal packing of $\gamma\delta$ resolvase subunits. *EMBO J 13*:1514–1524.

Sanderson MR, Freemont PS, Rice PA, Goldman A, Hatfull GF, Grindley NDF, Steitz TA. 1990. The crystal structure of the catalytic domain of the site-specific recombination enzyme $\gamma\delta$ resolvase at 2.7 Å resolution. *Cell 63*:1323–1329.

Stark WM, Grindley NDF, Hatfull GF, Boocock MR. 1991. Resolvase-catalysed reactions between *res* sites differing in the central dinucleotide of subsite I. *EMBO J 10*:3541–3548.

Stark WM, Sherratt DJ, Boocock MR. 1989. Site-specific recombination by Tn3 resolvase: Topological changes in the forward and reverse reactions. *Cell 58*:779–790.

Watson MA, Boocock MR, Stark WM. 1996. Rate and selectivity of synapsis of *res* recombination sites by Tn3 resolvase. *J Mol Biol 257*:317–329.

Weber DJ, Gittis AG, Mullen GP, Abeygunawardana C, Lattman EE, Mildvan AS. 1992. NMR docking of a substrate into the X-ray structure of staphylococcal nuclease. *Proteins Struct Funct Genet 13*:275–287.

Wishart DS, Sykes BD. 1994. The ^{13}C chemical-shift index: A simple method for identification of protein secondary structure using ^{13}C chemical shift data. *J Biomol NMR 4*:171–180.

Wüthrich K. 1986. *NMR of proteins and nucleic acids*. New York: Wiley.

Yang W, Steitz TA. 1995. Crystal structure of the site-specific recombinase γδ resolvase complexed with a 34 bp cleavage site. *Cell 82*:193–207.

Zhang O, Kay LE, Oliver JP, Forman-Kay JD. 1994. Backbone ^{1}H and ^{15}N resonance assignments of the N-terminal SH3 domain of drk in folded and unfolded states using enhanced-sensitivity pulsed field gradient NMR techniques. *J Biomol NMR 4*:845–858.